

H₂O megamasers: Accretion disks, jet interaction, outflows or massive star formation?

C. Henkel¹, J.A. Braatz², A. Tarchi^{3,4}, A.B. Peck⁵, N.M. Nagar⁶, L.J. Greenhill⁷, M. Wang⁸ and Y. Hagiwara⁹

¹*Max-Planck-Institut für Radioastronomie, Auf dem Hügel 69, D-53121 Bonn, Germany*

²*NRAO, P.O. Box 2, Green Bank, WV 24944, USA*

³*Istituto di Radioastronomia, CNR, Via Gobetti 101, I-40129 Bologna, Italy*

⁴*INAF-Osservatorio Astronomico di Cagliari, Loc. Poggio dei Pini, Strada 54, I-09012 Capoterra (CA), Italy*

⁵*Harvard-Smithsonian Center for Astrophysics, SAO/SMA Project, 645 N. A'ohoku Pl., Hilo, HI 96720, USA*

⁶*Kapteyn Instituut, Postbus 800, NL-9700 AV Groningen, The Netherlands*

⁷*Harvard-Smithsonian Center for Astrophysics, 60 Garden St., Cambridge MA 02138, USA*

⁸*Purple Mountain Observatory, Chinese Academy of Sciences, 210008 Nanjing, China*

⁹*ASTRON/Westerbork Radio Observatory, P.O. Box 2, NL-Dwingeloo 7990 AA, The Netherlands*

Abstract.

The 25 years following the serendipitous discovery of megamasers have seen tremendous progress in the study of luminous extragalactic H₂O emission. Single-dish monitoring and high resolution interferometry have been used to identify sites of massive star formation, to study the interaction of nuclear jets with dense molecular gas and to investigate the circumnuclear environment of active galactic nuclei (AGN). Accretion disks with radii of 0.1–3 pc were mapped and masses of nuclear engines of order 10⁶–10⁸ M_⊙ were determined. So far, ~50 extragalactic H₂O maser sources have been detected, but few have been studied in detail.

Keywords: masers



© 2018 Kluwer Academic Publishers. Printed in the Netherlands.

1. Introduction

To date, maser lines of five molecular species, those of CH, OH, H₂O, SiO, and H₂CO, have been detected in extragalactic space. While the number of observed OH masers, ~ 100 , is largest, the greatest emphasis of astrophysical research is focused on H₂O. This is a consequence of the fact that the 6₁₆–5₂₃ line of interstellar water vapor at 22.235 GHz ($\lambda \sim 1.3$ cm), first detected towards Orion-KL, Sgr B2 and W 49 (Cheung et al., 1969) and, outside the Galaxy, towards the nearby spiral M 33 (Churchwell et al., 1977), can be efficiently used to pinpoint sites of massive star formation and to elucidate the properties of active galactic nuclei (AGN). The line traces dense ($n(\text{H}_2) \gtrsim 10^7 \text{ cm}^{-3}$) warm ($T_{\text{kin}} \gtrsim 400$ K) molecular gas. Characteristic properties are enormous brightness temperatures ($\sim 10^{12}$ K has been measured), small sizes of individual hotspots ($\lesssim 10^{14}$ cm in galactic sources) and narrow linewidths (typically a few km s^{-1}) that make these masers to ideal probes of the structure and dynamics of the gas in which they reside. Because the apparent isotropic luminosity of these masers can be truly outstanding, reaching $10^{3-4} L_{\odot}$ (up to 10^{53} photons/s) in the most extreme cases, H₂O masers can be observed out to fairly large distances (up to $cz \sim 17700 \text{ km s}^{-1}$; Tarchi et al., 2003).

2. Kilomasers related to star formation

In the Galaxy, H₂O masers from star forming regions have isotropic luminosities of order $L_{\text{H}_2\text{O}} \lesssim 10^{-2} L_{\odot}$, with the notable exception of W 49 ($L_{\text{H}_2\text{O}} \sim 1 L_{\odot}$). The more luminous of these sources consist of a number of hotspots (see Brand et al., this volume). In nearby galaxies, masers with similar luminosities, the so-called kilomasers, are also found with luminosities up to a few L_{\odot} . Such masers are important to pinpoint sites of massive star formation (e.g. Tarchi et al., 2002) and to estimate distances on a purely geometric basis, comparing radial velocity and proper motion dispersions in groups of maser spots (Greenhill et al., 1993; Argon et al., 2004). Making use of known rotational properties, proper motions can also be used to determine three dimensional velocity vectors of entire galaxies (e.g. Brunthaler et al., 2002), thus providing information on the content and distribution of mass inside the Local Group.

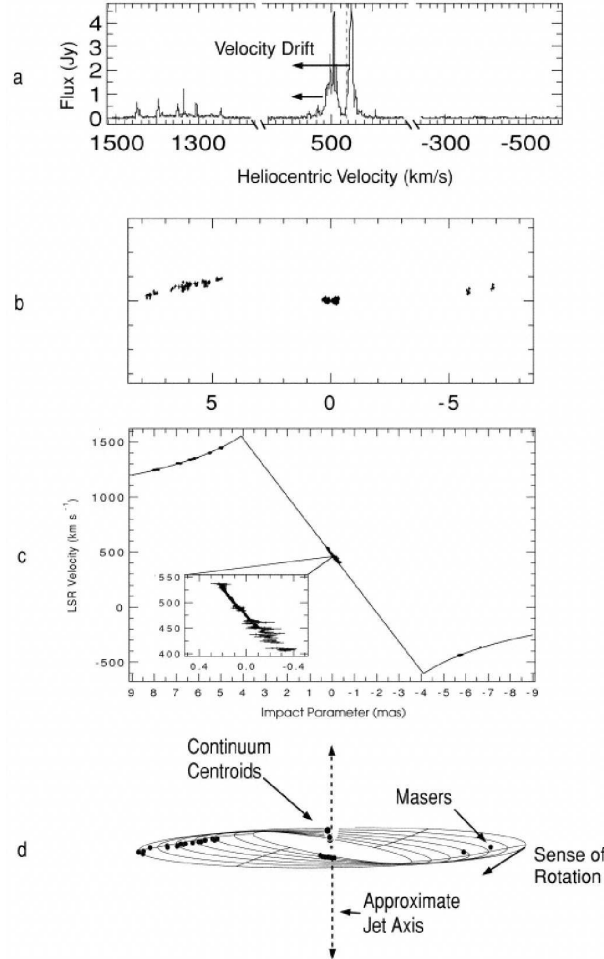


Figure 1. Overview of the NGC 4258 system: a) Typical spectrum, b) VLBA (Very Long Baseline Array) map, c) velocity versus impact parameter with Keplerian rotation curve fit, and d) warped disk with VLBA map (from Bragg et al. 2000).

3. Accretion disk megamasers

Megamasers, with $L_{\text{H}_2\text{O}} \gtrsim 20 L_{\odot}$, were first observed towards NGC 4945 (Dos Santos and Lépine, 1979) and then in NGC 1068, NGC 3079, NGC 4258 and the Circinus galaxy (Gardner and Whiteoak, 1982; Claussen et al., 1984; Henkel et al., 1984; Haschick and Baan, 1985). Two of these masers, those of NGC 1068 and NGC 4258, were soon found to be located in the innermost few parsecs of their parent galaxies (Claussen and Lo, 1986). Selection criteria to find more such masers as well as an interpretation of the molecular line emission in terms of properties

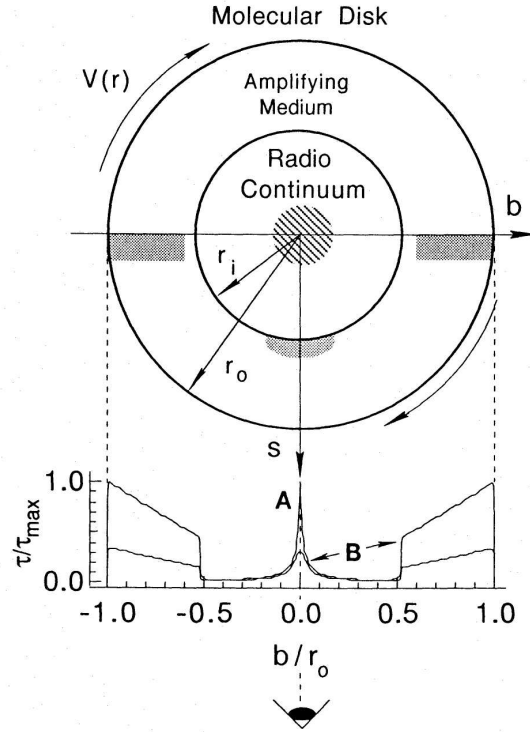


Figure 2. The Keplerian disk of NGC 4258 seen from above. The normalized optical depth along various lines of sight is shown for the plane of the disk, where b is the impact parameter. The shaded areas denote lines-of-sight with detected maser emission. r_i and r_o are the inner and outer radii of the masing disk, s marks the distance from its midline (from Greenhill et al. 1995a).

characterizing the nuclear environment of AGN remained, however, elusive for a full decade. A large survey including ~ 360 Seyfert and LINER galaxies (Braatz et al., 1996) finally led to the identification of another 10 megamasers, thus tripling the number of known sources and permitting, for the first time, a statistical analysis. All of these masers were found to be associated with Seyfert 2 or LINER nuclei (Braatz et al., 1997). Adopting the so-called unified scheme in which Seyfert 1s and 2s are identical except for angle of view, H_2O megamaser activity then is related to the large line-of-sight column densities expected when the nuclear tori are viewed edge-on. At least some LINER galaxies also contain large column densities of warm dense molecular gas as well as an AGN.

More detailed studies of the megamaser in NGC 4258 not only confirmed the presence of >10 systemic velocity features at a given time but also led to the detection of two additional H_2O velocity compo-

nents, $\pm 1000 \text{ km s}^{-1}$ off the systemic velocity (Nakai et al., 1993). The systemic features show a secular drift, with radial velocities increasing by $dV_s/dt \sim 10 \text{ km s}^{-1} \text{ yr}^{-1}$ (Haschick and Baan, 1990; Haschick et al., 1994; Greenhill et al., 1995a; Nakai et al., 1995). Very Long Baseline Interferometry (VLBI) reveals the presence of a warped edge-on Keplerian disk of $\sim 0.5 \text{ pc}$ diameter (Greenhill et al., 1995b; Miyoshi et al., 1995; Herrnstein et al., 1998a, Herrnstein et al., 1999), as shown in Fig. 1. Its geometry reflects the velocity coherence of the differentially rotating gas along the lines-of-sight towards its front side, its back side and its tangentially viewed regions (Fig. 2) as well as possible amplification of the radio continuum of the northern jet by the systemic features.

The positive velocity drift of the systemic component is readily explained by centripetal acceleration, implying that the features arise from the front and not from the back side of the masing disk (the latter would result in a negative drift). The ‘high velocity features’ originate from those parts of the disk seen tangentially. Applying the virial theorem yields

$$M_{\text{core}} = 1.12 \left[\frac{V_{\text{rot}}}{\text{km s}^{-1}} \right]^2 \left[\frac{R}{\text{mas}} \right] \left[\frac{D}{\text{Mpc}} \right] M_{\odot}, \quad (1)$$

with M_{core} being the mass enclosed by the Keplerian disk, V_{rot} denoting its rotational velocity at angular radius R , and D representing the distance to the galaxy. The VLBI maps allow us to directly measure V_{rot} and R for various values of R . From the Keplerian rotation curve we then obtain

$$C_1 = \left[\frac{V_{\text{rot}}}{\text{km s}^{-1}} \right] \left[\frac{R}{\text{mas}} \right]^{1/2}. \quad (2)$$

In addition, the observed E-W velocity gradient of the systemic features (Fig. 1c) provides

$$C_2 = \left[\frac{V_{\text{rot}}}{\text{km s}^{-1}} \right] \left[\frac{R}{\text{mas}} \right]^{-1}. \quad (3)$$

$C_1/C_2 = R^{3/2}$ then gives the angular radius R_s of the systemic features as viewed from a direction in the plane of the disk, but perpendicular to the line-of-sight. The result, $R_s \sim 4.1 \text{ mas}$, implies that the features are localized toward the inner edge of the disk. The distance to the disk, needed to estimate M_{core} in Eq. (1), is determined by measuring the centripetal acceleration

$$dV_s/dt = \frac{V_{\text{rot},s}^2}{r_s} = 9.3 \pm 0.3 \text{ km s}^{-1} \text{ yr}^{-1}. \quad (4)$$

With dV_s/dt and the rotational velocity $V_{\text{rot},s}$ of the systemic components known, the linear scale r_s can be compared with the angular

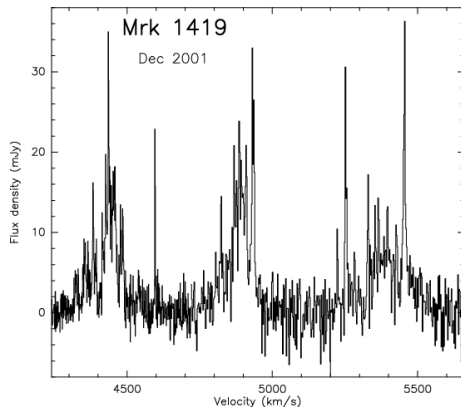


Figure 3. 22 GHz H₂O spectrum of Mrk 1419 (NGC 2960), taken with the 100-m telescope at Effelsberg (from Henkel et al. 2002) and showing the characteristic systemic (center), red- and blue-shifted groups of maser features.

scale, R_s , providing a measure of the distance. The proper motion of the individual systemic maser spots, $31.5 \pm 1.0 \mu\text{as yr}^{-1}$, allows, with $V_{\text{rot,s}}$ being known, a check of this distance estimate. The results of the two methods agree. $D = 7.2 \pm 0.5 \text{ Mpc}$ and $M_{\text{core}} = (3.9 \pm 0.3) \times 10^7 M_{\odot}$ within 0.14 pc (Herrnstein et al., 1999).

So far, all H₂O megamasers studied interferometrically arise from the innermost parsecs of their parent galaxy and all appear to be associated with AGN. Searching for NGC 4258-like targets showing three groups of H₂O features, one systemic, one red- and one blue-shifted, has become the Holy Grail of recent maser surveys. Such a configuration requires not only the presence of very dense molecular gas, but also a suitable viewpoint, with the nuclear disk seen almost edge-on. Therefore such sources are rarely found. Nevertheless, the number of detected sources falling into this category is steadily rising (see e.g. Fig. 3). Most notable are IC 2560 (2900 km s^{-1} ; Ishihara et al., 2001) and Mrk 1419 (4900 km s^{-1} ; Henkel et al., 2002). Very recently, four additional sources were identified, one at 7900 km s^{-1} (Braatz et al., 2004) and three at $>10000 \text{ km s}^{-1}$ (Greenhill et al., in preparation). Assuming that the model valid for NGC 4258 is generally applicable, single dish observations determining the drift of the systemic components (dV_s/dt) and the velocity offsets to the non-systemic components (V_{rot}) are sufficient for a rough estimate of the enclosed mass and linear scale of the disk. Thus it is possible to estimate angular scales of order 1 mas observing with resolutions of $35\text{--}40''$. So far, all measured centripetal accelerations are positive. The most plausible explanations are obscuration of the back side, perhaps by free-free absorption, and a lack of background radio continuum emission that could be amplified.

Maser dynamical masses (M_{core}) for a large sample of galaxies have the potential to establish the slope of the $M_{\text{core}}-\sigma$ relation and its intrinsic scatter (e.g. Ferrarese and Merritt, 2000), with uncertainties being dominated by the stellar velocity dispersion σ . Observing the three dimensional structure of a sample of accretion disks may provide strong constraints on heating (possibly irradiation by the nuclear X-ray source) and warping mechanisms (radiative torques have been proposed) and on the stability of these structures (e.g. Neufeld and Maloney, 1995). The thickness of the respective accretion disk is another important parameter (e.g. Moran et al., 1999), being crucial to calculations of accretion rate and identification of accretion modes (e.g. advective, convective, viscous). Determining the mass of the nuclear source, its distance, Eddington luminosity and accretion efficiency, the rate and mode of the nuclear accretion flow, the size and geometry of the nuclear disk or torus, the parent galaxy's deviation from the Hubble flow and calibrations of optical or near infrared indicators of distance with geometrically obtained values (see e.g. Eqs. 1–4) are all attractive goals.

In addition to the sources introduced above, there are a large number of targets exhibiting somewhat less regular spectra. These may either arise from tori that are unstable to fragmentation and star formation or from sources that combine an edge-on nuclear accretion disk with maser components of different nature that will be discussed below. Within this context, the most thoroughly studied sources are NGC 1068, NGC 3079 and the Circinus galaxy (Gallimore et al., 1996; Greenhill et al., 1996, Greenhill et al., 1997, Trotter et al., 1998; Hagiwara et al., 2002; Greenhill et al., 2003; Kondratko et al., 2004).

4. Jet megamasers

There are also sources in which at least a part of the H₂O emission is believed to be the result of an interaction between the nuclear radio jet and an encroaching molecular cloud. The first such source was NGC 1068, where not only the three groups of H₂O components from the accretion disk are seen (Greenhill et al., 1996), but where a fourth component is also detected. This originates from a region 0''3 (~ 30 pc) downstream, where the radio jet bends (Gallimore et al., 1996; Gallimore et al., 2001). To maximize detection rates of jet-maser sources, galaxies should be selected that either show evidence for interaction between the radio jet and clouds in the narrow line region or that show a face-on ($i < 35^\circ$) large scale galaxy disk and extended (up to 100 pc)

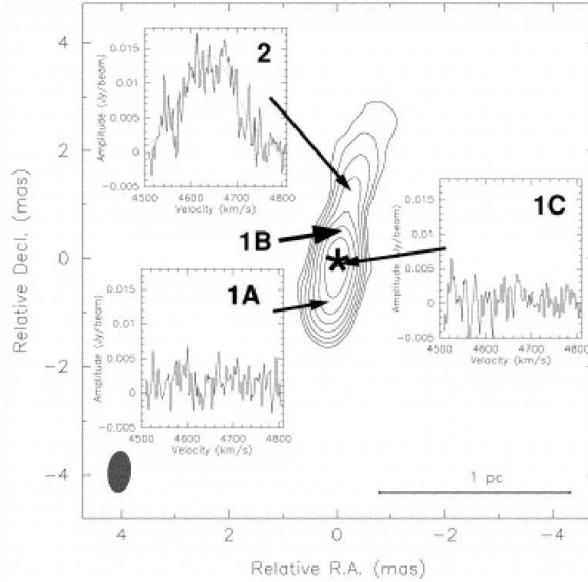


Figure 4. VLBA 22 GHz continuum and H₂O spectra towards Mrk 348 (NGC 262; see Peck et al. 2003). H₂O emission is only detected towards the northern jet.

radio structures, indicating that both the disk and the radio jet are fairly close to the plane of the sky.

Toward the elliptical galaxy NGC 1052 the H₂O maser features are located along the line-of-sight to the south-western nuclear jet (Claussen et al., 1998). In Mrk 348, a spiral galaxy with a particularly strong nuclear radio component, the megamaser appears to be associated with the northern jet (see Fig. 4; Peck et al., 2003). The intensity of the line emission is correlated with the continuum flux. The high linewidth ($\sim 130 \text{ km s}^{-1}$) on small spatial scales ($< 0.25 \text{ pc}$) and the rapid variability indicate that the H₂O emission is more likely to arise from a shocked region at the interface between the energetic jet and the ambient molecular gas than as a result of amplification of the continuum jet by molecular clouds along the line-of-sight. The line emission, red-shifted by 130 km s^{-1} with respect to the systemic velocity, may arise from gas being entrained by the receding jet. The close temporal correlation between the flaring activity of the maser and the continuum further suggests that the H₂O and continuum hotspots are nearly equidistant from the central engine and may be different manifestations of the same event.

5. New developments

Recently, optically detected large scale outflows were proposed to induce shocks that might trigger H₂O megamaser emission (Schulz and Henkel, 2003). Independently, it was found that in the Circinus galaxy the H₂O megamaser does not only trace a circumnuclear disk, but that there are also features associated with a wide angle outflow (Greenhill et al., 2003). H₂O maser emission traces this outflow out to 1 pc from the central engine with line-of-sight velocities up to $\pm 160 \text{ km s}^{-1}$ w.r.t. systemic. The outflowing wind is observed in those regions around the circumnuclear disk that are not shadowed by its warp. The position angles of the edges of the outflow correspond to those of the outflow and ionization cones observed at radio and optical wavelengths on much larger scales (Veilleux and Bland-Hawthorn, 1997; Curran et al., 1999). Thus in addition to accretion disk and jet megamasers, strong maser emission can also be associated with large scale nuclear outflows. Yet another kind of H₂O megamaser might be associated with massive star formation. So far there is not yet a confirmed source. Towards Arp 299, an interacting pair of galaxies, luminous H₂O megamaser emission was detected that might be associated with star formation in the overlapping region between its main members NGC 3690 and IC 694 (Peck et al., 2004). This possibility has, however, to be confirmed by interferometric measurements.

As suggested by Sect. 2, most H₂O kilomasers are associated with star formation. There are, however, exceptions. Towards M 51, the kilomaser was found to coincide with the nucleus within 250 mas (~ 10 pc; Hagiwara et al., 2001). A similarly good coincidence, within $1''$ (~ 12 pc), was also found for the main maser component in the starburst galaxy NGC 253 (Henkel et al., 2004). The nature of these sources that are too weak to be seen at distances well in excess of 10 Mpc is still under discussion.

Almost a decade ago, all H₂O megamasers were found to be associated with Seyfert 2 and LINER galaxies (Braatz et al., 1997). In the meantime, however, with a much larger number of detections, the situation has become more complex. While megamasers are detected in optically ‘normal’ galaxies (Greenhill et al., 2002), a particularly luminous megamaser was recently found in the FRII radio galaxy 3C 403 (Tarchi et al., 2003). Another megamaser host, NGC 5506, was identified as a Narrow Line Seyfert 1 (Nagar et al., 2002). The detection of a nuclear kilomaser in a second such galaxy, NGC 4051 (Hagiwara et al., 2003), was interpreted in terms of a relatively low inclination of the nuclear disk or torus w.r.t Seyfert 2 galaxies, thus yielding relatively low column densities for coherent amplification. Even more recently,

H₂O was detected in the prototypical Seyfert 1 NGC 4151 (Braatz et al., 2004). It is still too early for a detailed interpretation, but it is clear that these detections will be essential for a better understanding of the unifying scheme differentiating between type 1 and type 2 AGN.

Is there a way to predict the presence of H₂O megamasers by observations at other wavelengths? This question was recently discussed for the prototypical sources NGC 1068, NGC 3079 and NGC 4258 (Bennert et al., 2004). All three galaxies exhibit a spatially compact ($\lesssim 1''$) near infrared core containing dust clouds that are heated by the central engine. This appears to be the main hint for the potential presence of accretion disk masers, but these cores are more difficult to detect than the masers themselves. Tracers for jet masers at optical and near infrared wavelengths are spectral lines that are split into two velocity components.

6. Future projects

Though the sensitivity of existing facilities can be slightly enhanced, order(s) of magnitude improvements will only be possible with the Square Kilometer Array (SKA), complemented by space interferometry to combine optimal sensitivity with optimal angular resolution. The 22 GHz line of water vapor bears the prospect to reveal the magnetic field strength through its Zeeman pattern. A measurement towards NGC 4258 yielded a 1σ upper limit of 300 mG for the toroidal component (Herrnstein et al., 1998b). Probably only the SKA will provide the sensitivity to determine the magnetic field in the circumnuclear environment of active galaxies. The same may hold for searches of H₂O megamasers at cosmological redshifts. On the other hand, accounting for the statistical properties of detected maser sources, it appears that existing facilities have the potential to drastically enlarge the number of known luminous sources of H₂O emission. So far, possibly only a small percentage of the detectable megamasers have been found (Peck et al., 2004).

References

- Argon, A.L., Greenhill, L.J., Reid, M.J. et al. 2004, *ApJ*, submitted
 Bennert, N., Schulz, H. and Henkel, C. 2004, *A&A*, **419**, 127
 Braatz, J.A., Wilson, A.S. and Henkel, C. 1996, *ApJS*, **106**, 51
 Braatz, J.A., Wilson, A.S. and Henkel, C. 1997, *ApJS*, **110**, 321
 Braatz, J.A., Henkel, C., Greenhill, L.J., Moran, J.M. and Wilson, A.S. 2004, *ApJ*, in preparation

- Bragg, A.E., Greenhill, L.J., Moran, J.M. and Henkel, C. 2000, *ApJ*, **535**, 73
- Brunthaler, A., Falcke, H., Reid, M., Greenhill, L.J. and Henkel, C. 2002, *Proc. of the 6th European VLBI Symp.*, eds. Ros et al., MPIfR, Bonn, Germany, p. 189
- Cheung, A.C., Rank, D.M., Townes, C.H., Thornton, D.D. and Welch, W.J. 1969, *Nature*, **221**, 626
- Churchwell, E., Witzel, A., Huchtmeier, W., et al. 1977, *A&A*, **54**, 969
- Claussen, M.J., Heiligman, G.M. and Lo, K.-Y. 1984, *Nature*, **310**, 298
- Claussen, M.J. and Lo, K.-Y. 1986, *ApJ*, **308**, 592
- Claussen, M.J., Diamond, P.J., Braatz, J.A., Wilson, A.S., and Henkel, C. 1998, *ApJ*, **500**, L129
- Curran, S.J., Rydbeck, G., Johansson, L.E.B. and Booth, R.S. 1999, *A&A*, **344**, 767
- Dos Santos, P.M. and Lépine, J.R.D. 1979, *Nature*, **278**, 34
- Ferrarese, L. and Merritt, D. 2000, *ApJ*, **539**, L9
- Gardner, F.F. and Whiteoak, J.B. 1982, *MNRAS*, **201**, 13p
- Gallimore, J.F., Baum, S.A., O’Dea, C.P., Brinks, E. and Pedlar, A. 1996, *ApJ*, **462**, 740
- Gallimore, J.F., Henkel, C., Baum, S.A., et al. 2001, *ApJ*, **556**, 694
- Greenhill, L.J. and Gwinn, C.R. 1997, *ApSS*, **248**, 261
- Greenhill, L.J., Moran, J.M., Reid, M.J., Menten, K.M. and Hirabayashi, H. 1993, *ApJ*, **406**, 482
- Greenhill, L.J., Henkel, C., Becker, R., Wilson, T.L. and Wouterloot, J.G.A. 1995a, *A&A*, **304**, 21
- Greenhill, L.J., Jiang, D.R., Moran, J.M., et al. 1995b, *ApJ*, **440**, 619
- Greenhill, L.J., Gwinn, C.R., Antonucci, R. and Barvainis, R. 1996, *ApJ*, **472**, L21
- Greenhill, L.J., Ellingsen, S.P., Norris, R.P. et al. 2002, *ApJ*, **565**, 836
- Greenhill, L.J., Booth, R.S., Ellingsen, S.P., et al. 2003, *ApJ*, **590**, 162
- Hagiwara, Y., Henkel, C., Menten, K.M. and Nakai, N. 2001, *ApJ* **560**, L37
- Hagiwara, Y., Henkel, C., Sherwood, W.A. and Baan, W.A. 2002, *A&A* **387**, L29
- Hagiwara, Y., Diamond, P.J., Miyoshi, M., Rovilos, E. and Baan, W.A. 2003, *MNRAS* **344**, L53
- Haschick, A.D. and Baan, W.A. 1985, *Nature* **314**, 144
- Haschick, A.D. and Baan, W.A. 1990, *ApJ* **355**, L23
- Haschick, A.D., Baan, W.A. and Peng, E.W. 1994, *ApJ* **437**, L35
- Henkel, C., Güsten, R., Downes, D., et al. 1984, *A&A*, **141**, L1
- Henkel, C., Braatz, J.A., Greenhill, L.J. and Wilson, A.S. 2002, *A&A*, **394**, L23
- Henkel, C., Tarchi, A., Menten, K.M. and Peck, A.B. 2004, *A&A*, **414**, 117
- Herrnstein, J.R., Greenhill, L.J., Moran, J.M., et al. 1998a, *ApJ*, **497**, L69
- Herrnstein, J.R., Moran, J.M., Greenhill, L.J., Blackman, E.G. and Diamond, P.J. 1998b, *ApJ*, **508**, 243
- Herrnstein, J.R., Moran, J.M., Greenhill, L.J., et al. 1999, *Nature*, **400**, 539
- Ishihara, Y., Nakai, N., Iyamoto, N., et al. 2001, *PASJ*, **53**, 215
- Kondratko, P.T., Greenhill, L.J. and Moran, J.M. 2004, *ApJ*, in preparation
- Miyoshi, M., Moran, J.M., Herrnstein, J.R., et al. 1995, *Nature*, **373**, 127
- Moran, J.M., Greenhill, L.J., Herrnstein, J.R. 1999, *JApA*, **20**, 165
- Nagar, N.M., Oliva, E., Marconi, A. and Maiolino, R. 2002, *A&A*, **391**, L21
- Nakai, N., Inoue, M. and Miyoshi, M. 1993, *Nature*, **361**, 45
- Nakai, N., Inoue, M., Miyazawa, K., Miyoshi, M. and Hall, P. 1995, *PASJ*, **47**, 771
- Neufeld, D.A. and Maloney, P.R. 1995, *ApJ*, **447**, L17
- Peck, A.B., Henkel, C., Ulvestad, J.S., et al. 2003, *ApJ*, **590**, 149
- Peck, A.B., Tarchi, A., Henkel, C., et al. 2004, *ApJ*, in preparation
- Schulz, H. and Henkel, C. 2003, *A&A*, **400**, 41

- Tarchi, A., Henkel, C., Peck, A.B. and Menten, K.M. 2002, *A&A*, **389**, L39
Tarchi, A., Henkel, C., Chiaberge, M. and Menten, K.M. 2003, *A&A*, **407**, L33
Trotter, A.S., Greenhill, L.J., Moran, J.M., et al. 1998, *ApJ*, **495**, 740
Veilleux, S. and Bland-Hawthorn, J. 1997, *ApJ*, **479**, L105

Address for Offprints: Max-Planck-Institut für Radioastronomie
Auf dem Hügel 69
D-53121 Bonn
Germany